Optics Communications 443 (2019) 197–201

Contents lists available at ScienceDirect

Optics Communications

journal homepage: www.elsevier.com/locate/optcom

The directional excitation of surface plasmon polaritons by radially polarized beam with multiple off-axis vortices

YuXin Dong [a,b], SiXing Xi [c], BoWen Zhu [a], XiaoLei Wang [a,b,*], QuanQuan Mu [b], Shuai Wang [a], ZhuQing Zhu [d]

[a] Institute of Modern Optics, Nankai University, Tianjin 300350, China
[b] State Key Laboratory of Applied Optics, Changchun Institute of Optics, Fine Mechanics and Physics, Chinese Academy of Sciences, Changchun, 130033, China
[c] School of Science, Hebei University of Engineering, Handan, Hebei 056038, China
[d] Key Laboratory of Optoelectronic Technology of Jiangsu Province, School of Physical Science and Technology, Nanjing Normal University, Nanjing 210023, Jiangsu, China

ARTICLE INFO

Keywords:
Polarization
Optical vortices
Subwavelength structures
Laser beam shaping
Surface plasmons

ABSTRACT

A method of directional excitation of surface plasmon polaritons (SPPs) is proposed by using radially polarized beam loaded with multiple off-axis vortices. Based on the Kretschmann–Raether three-layer structure, the theory expression for the distribution of SPPs on the silver film surface excited by the radially polarized beam loaded with multiple off-axis vortices is derived. Accordingly, the influence of multiple off-axis vortices on the distribution of focus field and SPPs is analyzed, in which the asymmetry of the SPPs caused by the off-axis vortex is found out. On this basis, the SPPs are directionally excited by adjusting the arrangement and position of multiple off-axis vortices reasonably. This work demonstrated that the off-axis vortices introduce a new degree of freedom for SPPs manipulation, and that the excitation and propagation of SPPs can be dynamically controlled by judiciously arranging the multiple off-axis vortices. Without specially designed metal structures, the all-optical controlled method for SPPs manipulation has great potential in plasmonic tweezers and plasmonic devices.

1. Introduction

Surface plasmon polaritons (SPPs) are electromagnetic waves propagating along the metal/dielectric interface, whose intensity is suppressed in the direction of the vertical surface in the form of exponential decay. SPPs have attracted many attentions due to their special properties: shorter wavelength than that of the excitation beam, high electric field confinement and enhancement, high sensitivity to the variation of refractive index of the dielectric [1,2]. These exceptional features of SPPs have a variety of advanced applications including ultra-diffraction limit resolution imaging [3,4], micro–nano processing [5,6], particle manipulation [7], biosensor [8,9], plasmon waveguide [10–12] and plasmon lens (slit-grating lens [13], concentric ring lenses [14–16], microporous array lenses [17], etc.).

Recently, the effective directional excitation of SPPs has received much attention. Several novel designs have been proposed in which the key is the intervention of an asymmetry, either in structural or in illumination system. For example, the Bragg grating is applied to block the propagation of unilateral SPPs [18], but the unidirectional SPPs do not switch the propagation direction. On one hand, the symmetrical structure irradiated by asymmetric incident light is proposed and the propagation direction of the SPPs can be controlled by changing the angle of the incident light [19–21], not only that, dynamically controlling the direction of SPPs also can be achieved on a designed two thin slit structure by simply modulating the phase difference between the incident dual fundamental Gaussian beams [22]. On the other hand, a series of asymmetrical structures, such as metal trough array [23], double slit [24], groove [25], T-shaped structure [26], magnetic dipole antenna [27] are proposed with symmetric irradiation, in which the directional excitation of SPPs is achieved by changing the parameters of the asymmetry structure. However, most of these previous works were based on the specially designed structure, which restricted the practical applications of SPPs due to the complex production process of the structure, large loss of light scattering and absorption of the structure and difficulty of reconstruction.

SPPs can be effectively excited when the incident light is TM polarization with respect to the metal interface. Hence, ordinary light causes non-TM polarization energy loss in excitation of SPPs. A very strong longitudinal field (TM polarization) can be obtained when the radially polarized beam is tightly focused by a high numerical aperture objective [28], which not only greatly improves the excitation efficiency of

* Corresponding author at: Institute of Modern Optics, Nankai University, Tianjin 300350, China.
E-mail address: wangxiaolei@nankai.edu.cn (X. Wang).

https://doi.org/10.1016/j.optcom.2019.03.050
Received 5 December 2018; Received in revised form 14 March 2019; Accepted 20 March 2019
Available online 22 March 2019
0030-4018/

SPPs [29,30], but also effectively reduces the noise caused by other components. The intensity profile of the focused vortex beam is an annular structure and the intensity of the concentric rings gradually decreases with increasing radius, while there is a "dark field" in the center of light propagation where the light intensity always remains zero. Therefore, in view of the current research status of directional excitation of SPPs discussed above, combined with the unique properties of radially polarized beam and optical vortex, a method for directional excitation of SPP by using radially polarized beam loaded with multiple off-axis vortices is proposed in this paper, in which the tight focus distribution can be adjusted by properly designing the arrangement of multiple off-axis vortices and thus the symmetry of SPPs in air/metal interface is broken. Theoretical analysis and numerical simulations demonstrate that the off-axis vortices introduce a new freedom degree for manipulation of SPPs, and the excitation and propagation of SPPs can be controlled by judiciously arranging the multiple off-axis vortices. In addition, dynamic manipulation of SPPs can be realized when spatial light modulator is used to load the vortices on incident vector beam. Without specially designed metal structures, the all-optical controlled method for SPPs manipulation has great potential in plasmonic tweezers and plasmonic devices.

2. Principle

Kretschmann–Raether configuration is adopted to illustrate the excitation of SPPs and the schematic is shown in Fig. 1. The configuration comprises of a lens and three-layer system. The lens is a high numerical aperture oil immersion objective ($n_{oil} = 1.515$). The three-layer system is a thin silver film (with thickness d_2 of 50 nm and dielectric constant of ($\varepsilon_{silver} = n_2^2 = -7.9 + 0.736i$) sandwiched between glass ($n_{glass} = n_1 = 1.515$) and air ($n_{air} = n_3 = 1$). A larger convergence angle $\theta_{\max}$ was provided by the lens that focuses the incident beam onto the glass–silver film interface located at the focal plane. The incident beam which satisfied the wave vector matching condition can excite the SPPs effectively in the silver film–air interface, that is, $\theta_{\max} \geq \theta_{spps}$, where θ_{spps} is the excitation angle of SPPs.

The electric field of SPPs excited on the silver film in microscopic configuration can be calculated with the Richards–Wolf vector diffraction theory when it is focused by a high NA lens. The field components of SPPs in the air above the silver film can be derived as [31]

$$\vec{E}_{out} = \begin{pmatrix} E_{n_3\_r} \\ E_{n_3\_\varphi} \\ E_{n_3\_z} \end{pmatrix} = -\frac{jfk_3}{2\pi}\int_0^{2\pi}\int_0^{\alpha} P(\theta_1)\,A(\theta_1)\sin\theta_1 \times \begin{pmatrix} t_r{}^p\left[\sin(\sigma-\phi)\sin(\phi-\varphi)+\cos(\sigma-\phi)\cos\theta_1\cos(\phi-\varphi)\right] \\ t_\varphi{}^s\left[\sin(\sigma-\phi)\cos(\phi-\varphi)+\cos(\sigma-\phi)\cos\theta_1\sin(\phi-\varphi)\right] \\ -t_z{}^p\cos(\sigma-\phi)\sin\theta_1 \end{pmatrix} \times \exp\left[jz\sqrt{k_3{}^2-k_1{}^2\sin\theta_1{}^2}+j\left(k_1 r\sin\theta_1\cos(\varphi-\phi)\right)\right] d\phi d\theta_1 \tag{1}$$

where f is the focal length of the lens, α is the convergence semiangle, $P(\theta_1)$ is the apodization function and $A(\theta_1)$ represents the amplitude and phase distribution of the incident beam, k_1 and k_3 represent the wave vectors in the glass and air, respectively. σ is a function determining the polarization mode that $\sigma = n\phi$, in which n represents the degree of polarization of the vector beam (n is an integer) [14], for the radially polarized beam, $\sigma = \phi$.$t_r{}^p$, $Pt_\varphi{}^s$ and $t_z{}^p$ represent the transmission coefficient of $E_{n_3\_r}$, $E_{n_3\_\varphi}$ and $E_{n_3\_z}$ components through the silver film respectively, and they can be expressed as:

$$t_r{}^p = \frac{\sqrt{\varepsilon_3-\varepsilon_1\times\sin^2\theta}}{\sqrt{\varepsilon_3}\cos\theta}\times\frac{t_{12}^p t_{23}^p\exp(jk_{z2}d_2)}{1+r_{12}^p r_{23}^p\exp(j2k_{z2}d_2)} = \frac{\sqrt{k_3{}^2-k_1{}^2\times\sin^2\theta}}{k_3\cos\theta}\times t^p \tag{2}$$

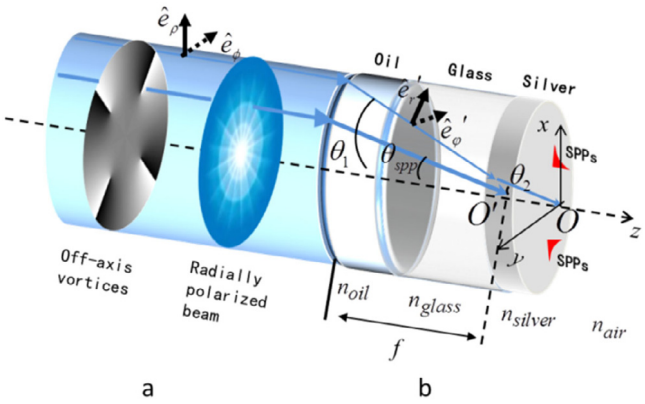

Fig. 1. (a) Incident radially polarized beam loaded with off-axis vortices. (b) Schematic diagram of the Kretschmann–Raether configuration, in which the incident beam is focused on the silver film surface of the glass–silver film–air dielectric layer by high numerical aperture oil immersion lens.

$$t_r{}^s = \frac{t_{12}^s t_{23}^s\exp(jk_{z2}d_2)}{1+r_{12}^s r_{23}^s\exp(j2k_{z2}d_2)} = t^s \tag{3}$$

$$t_z{}^p = \frac{\sqrt{\varepsilon_1}}{\sqrt{\varepsilon_3}}\times\frac{t_{12}^p t_{23}^p\exp(jk_{z2}d_2)}{1+r_{12}^p r_{23}^p\exp(j2k_{z2}d_2)} = \frac{k_1}{k_3}\times t^p \tag{4}$$

where t^p and t^s respectively represent the transmission coefficient of the p- and s-polarization component through the silver film at the incident angle of θ_1, t_{ij}^s and t_{ij}^p are the Fresnel transmission coefficients for s- and p-polarization at the i/j interface, and r_{ij}^s, r_{ij}^p are the corresponding reflection coefficients, k_{z2} denotes the z-component of wave vector within the metal film, and d is the metal film thickness, respectively.

Assume the system obeys the sine condition, $P(\theta_1) \propto \sqrt{\cos\theta_1}$ in Eq. (1) [32]. $A(\theta_1)$ is replaced by E_{in} which respects the radially polarized beam with multiple off-axis vortices. Thus, the field component of the SPPs can be derived as

$$\vec{E}_{\rho\_out} = \begin{pmatrix} E_{\rho\_n_3\_r} \\ E_{\rho\_n_3\_\varphi} \\ E_{\rho\_n_3\_z} \end{pmatrix} = -\frac{jfk_3}{2\pi}\int_0^{\alpha}\int_0^{2\pi}\sqrt{\cos\theta_1}E_{in}\sin\theta_1 \times \begin{pmatrix} t^p\dfrac{\sqrt{k_3{}^2-k_1{}^2\sin\theta_1{}^2}}{k_3}\cos(\phi-\varphi) \\ t^s\cos\theta_1\sin(\phi-\varphi) \\ -t^p\dfrac{k_1}{k_3}\sin\theta_1 \end{pmatrix} \times \exp\left[jz\sqrt{k_3{}^2-k_1{}^2\sin\theta_1{}^2}+\left(jk_1 r\sin\theta_1\cos(\varphi-\phi)\right)\right] d\theta_1 d\phi \tag{5}$$

The expression of the incident radially polarized beam loaded with multiple off-axis vortices whose locations are P_1, $P_2 \ldots P_N$ with topological charge (TC) m_1, $m_2 \ldots m_N$ can be expressed as [33]

$$\begin{aligned}\vec{E}_{in} &= \vec{E}_{in\_\rho}(\rho e^{j\phi}-\rho_1 e^{j\phi_1})^{m_1}(\rho e^{j\phi}-\rho_2 e^{j\phi_2})^{m_2}\ldots(\rho e^{j\phi}-\rho_N e^{j\phi_N})^{m_N} \\ &= \vec{E}_{in\_\rho}\sum_{l=0}^{L}A_{L-l}\rho^l e^{jl\phi}\end{aligned} \tag{6}$$

by taking

$$L = \sum_{n=1}^{N} m_n \tag{7}$$

where A_{L-l} represents the expansion factor.

Taking Eq. (6) into Eq. (5), SPPs distribution on interface between the silver film and the air under illumination of the radially polarized

beam with multiple off-axis vortices can be obtained as follow:

$$\vec{E}_{\rho\_out} = -\frac{jfk_3}{2\pi}\sum_{l=0}^{L} A_{L-l}\exp(jl\phi)\int_0^{\alpha}\int_0^{2\pi}\sqrt{\cos\theta_1}E_{in\_\rho}\rho^l\sin\theta_1 \times\begin{pmatrix} t^p\dfrac{\sqrt{k_3{}^2-k_1{}^2\sin\theta_1{}^2}}{k_3}\cos(\phi-\varphi) \\ t^s\cos\theta_1\sin(\phi-\varphi) \\ -t^p\dfrac{k_1}{k_3}\sin\theta_1 \end{pmatrix} \times\exp\left[jz\sqrt{k_3{}^2-k_1{}^2\sin\theta_1{}^2}+\left(jk_1r\sin\theta_1\cos(\varphi-\phi)\right)\right]d\theta_1 d\phi \tag{8}$$

According to the integral transformation formula of n-order Bessel formula

$$\int_0^{2\pi}\exp\left[ik_1r\sin\theta_1\cos\phi-m\phi\right]d\phi = 2\pi i^n J_n(k_1r\sin\theta_1)$$
$$J_{-n}(k_1r\sin\theta_1) = (-1)^n J_n(k_1r\sin\theta_1) \tag{9}$$

The SPPs distribution excited in the silver film and air interface can be finally derived as

$$\vec{E}_{\rho\_out} = -\frac{fk_3}{2}\sum_{l=0}^{L} A_{L-l}j^l\exp(jl\varphi)\int_{\theta_{\min}}^{\theta_{\max}}\sqrt{\cos\theta_1}E_{in\_\rho}\rho^l\sin\theta_1 \times\begin{pmatrix} t^p\dfrac{\sqrt{k_3{}^2-k_1{}^2\sin\theta_1{}^2}}{k_3}\left[J_{l+1}(k_1r\sin\theta_1)-J_{l-1}(k_1r\sin\theta_1)\right] \\ -jt^s\cos\theta_1\left[J_{l+1}(kr\sin\theta_1)-J_{l-1}(k_1r\sin\theta_1)\right] \\ 2jt^p\dfrac{k_1}{k_3}\sin\theta_1 J_l(k_1r\sin\theta_1) \end{pmatrix} \times\exp\left(jz\sqrt{k_3{}^2-k_1{}^2\sin\theta_1{}^2}\right)d\theta_1 \tag{10}$$

where the upper and lower points $\theta_{\max}$ and $\theta_{\min}$ are the corresponding angle values of $\theta_{spp}(1\pm10\%)$, respectively. θ_{spp} denotes the excitation angle of the SPPs satisfying the wave vector matching condition. As long as the light converged by the maximum angle satisfies $\alpha > \theta_{spp}$, the incident beam can effectively excite the SPPs on the metal surface.

3. Numerical results

According to Eq. (10), the excitation of SPPs by radially polarized beam loaded with single off-axis vortex and multiple off-axis vortices are studied consecutively by numerical simulation in this section. Beam waist of 2.56 mm and wavelength of 488 nm are adopted for the simulations, the topological charge of the vortex is all m = 1 and the off-axis distance is $r_0 = 0.5w$.

3.1. SPPs excited by symmetric multiple off-axis vortices

Fig. 2 shows the SPPs distribution on the silver film–air surface excited by the radially polarized beam with symmetric multiple-vortices. The first column shows the arrangements of off-axis vortices in the incident field. The second to the fourth columns are the azimuthal, radial and longitudinal components of SPPs in the x-y plane, respectively. It can be seen that the proportion of the longitudinal component is the largest and the azimuthal component is the smallest, and the difference in three orders of magnitude between them can be found. The maximum energy between longitudinal components and the radial components is close to one order of magnitude. The fifth column is the total field distribution of SPPs in the x-y plane, which is similar to the distribution of the longitudinal components shown in the third column.

As shown in the first row of Fig. 2, when a single center vortex is loaded in incident beam, the SPPs are clustered from the periphery to the center symmetrically and form a complete ring with symmetry. Compared with the single center vortex, the second row in Fig. 2 shows

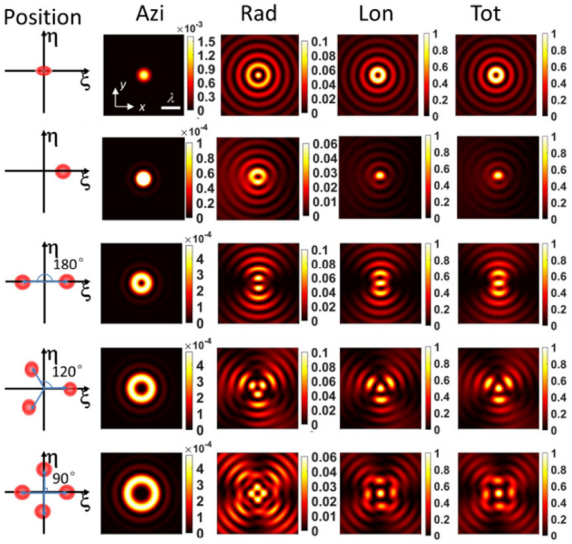

Fig. 2. The SPPs distribution on silver film–air surface excited by radially polarized beam loaded with vortices. From left to right, they are the arrangements of the vortices, the azimuthally component, the radial component, the longitudinal component and the total field distribution of SPPs in the x-y plane, respectively.

that the symmetry and integrality of SPPs are broken, which laid the foundation to achieve controllable excitation direction of SPPs. When the multiple off-axis vortices are loaded(second to fifth rows in Fig. 2), the radial and longitudinal components have a broken structure with multiple side lobes and the broken parts have no SPPs distribution, in order to achieve the unidirectional SPP. By changing the position of the loaded vortex, the position of the broken structure can also be changed, that is, the direction of the excited SPPs also changes, thus resulting the regulation of the direction of excited SPPs. The azimuthal component did not have a broken distribution because there was no TM component that could excite SPPs. The side lobes of SPPs increase as the number of vortices increases, and the number of side lobes equals the number of vortices. In this way, the SPPs distribution follows the arrangements of multiple off-axis vortices and the excitation of SPPs in any direction can be achieved by rotating the multi-vortex array as a whole.

In this method, the asymmetric distribution of SPPs is achieved due to the redistribution of focal field induced by the existence of vortices. The off-axis vortices induced redistribution of focal field and rotation of energy flow were discussed detailly in our previous published paper [33]. By Fig. 2, we find that the angular intervals corresponding to any two adjacent vortices are equal, and the angular interval becomes smaller as the number of vortices increases. Therefore, the assumption that the asymmetric distribution of SPPs induced by the off-axis vortex can be affected by the change of angular interval of two adjacent vortices is proposed and verified below.

3.2. SPPs excited by asymmetric multiple off-axis vortices

As shown in Fig. 3, the case that number of vortices are N = 2, 3, 4, and 8 are numerical simulated and analyzed, respectively. The arrangement of vortices in the first column is as follows: taking the positive x-axis as the starting position of the vortex and controlling the angular interval of the vortices $\theta_{\text{gap}} = \pi/N, \pi/2N, \pi/3N, 0$, the corresponding distributions of the excited SPPs are shown in the second column to the five columns. The results of each line in Fig. 3 show that the excited SPPs appeared to diffuse. The reason for this phenomenon is that the energy flow in the focal field caused by the vortex is rotated. When the angular interval is reduced, the direction which diffusion occurs rotates clockwise toward the vortex accumulation, resulting change of the direction of the excited SPPs. Therefore, the numerical

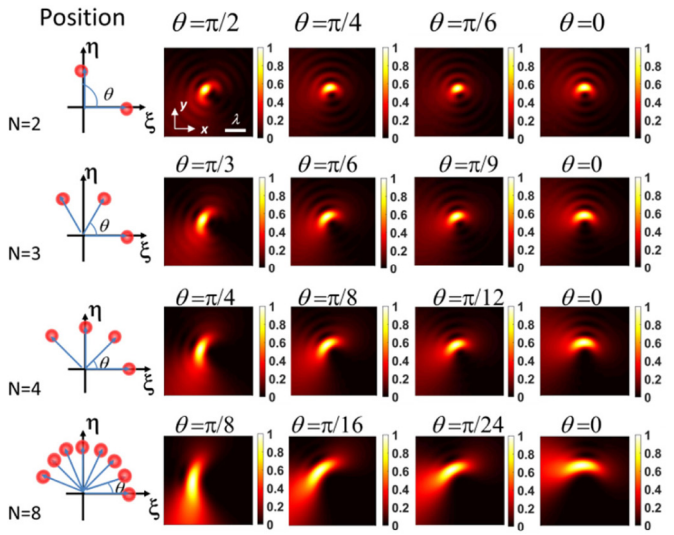

Fig. 3. The SPPs field distribution excited by asymmetrically arranged off-axis vortices. From left to right are the arrangements of the multiple vortices with equal angular separation and the distribution of the total of SPPs in x-y plane at different angular intervals, respectively. N is the number of vortices and θ is the interval angle between two adjacent vortices.

simulations demonstrated that the changes in the angular interval indeed have an impact on SPPs excitation. By changing the angular interval, the direction of the excited SPPs can be changed so as to achieve the directional excitation of the SPPs. Further, from the second to the fourth columns in Fig. 3, it is easy to find that the diffusion length of SPPs increases with the number of vortices increases. This method of controlling the directional excitation of SPPs relies mainly on diffusion of vortex.

4. Conclusion

In conclusion, we studied the SPPs on the air–silver interface excited by the radially polarized beam loaded with multiple off-axis vortices and achieved directional excitation of SPPs by changing the number and positions of off-axis vortices. The formula for the distribution of SPPs on the silver film surface excited by the radially polarized beam loaded with off-axis vortices is derived. This work demonstrated that the off-axis vortices introduce a new freedom degree for manipulation of SPPs, and the excitation and propagation of SPPs can be controlled by judiciously arranging the multiple off-axis vortices. In this method, the excitation efficiency of SPPs was improved due to the application of radially polarized beam and the off-axis vortex is employed to break the symmetry distribution of focusing field so that the directional excitation of SPPs has been achieved, which has the advantages of flexibility and easy operation. In addition, dynamic manipulation of SPPs can be realized when spatial light modulator is used to load the vortices on incident vector beam. This all-optical unstructured method for SPPs directional excitation has great potential in super-resolution imaging, micro/nano processing, particle manipulation and biological sensing.

Acknowledgment

We are particularly grateful to Professor Qiwen Zhan (University of Dayton, USA) for his helpful discussions.

Funding information

The authors acknowledge the funding support from National Natural Science Foundation of China (NSFC) (No. 61875093) and the State Key Laboratory of Applied Optics, China.

References

[1] W.H. Weber, G.W. Ford, Optical electric-field enhancement at a metal surface arising from surface-plasmon excitation, Opt. Lett. 6 (3) (1981) 122–124, http://dx.doi.org/10.1364/OL.6.000122.
[2] W.L. Barnes, A. Dereux, T.W. Ebbesen, Surface plasmon subwavelength optics, Nature 14 (424) (2003) 824–830, http://dx.doi.org/10.1038/nature01937.
[3] N. Fang, H. Lee, C. Sun, X. Zhang, Sub-diffraction-limited optical imaging with a silver superlens, Science 308 (5721) (2005) 534–537, http://dx.doi.org/10.1126/science.1108759.
[4] D.R. Smith, D. Schurig, M. Rosenbluth, S. Schultz, S.A. Ramakrishna, J.B. Pendry, Limitations on subdiffraction imaging with a negative refractive index slab, Appl. Phys. Lett. 82 (2003) 1506, http://dx.doi.org/10.1063/1.1554779.
[5] X.G. Luo, T. Ishihara, Subwavelength photolithography based on surface-plasmon polariton resonance, Opt. Express 12 (14) (2004) 3055–3065, http://dx.doi.org/10.1364/OPEX.12.003055.
[6] L. Pan, Y. Park, Y. Xiong, U.A. Erick, W. Yuan, Z. Li, X. Shaomin, R. Junsuk, S. Cheng, B.B. David, Z. Xiang, Maskless plasmonic lithography at 22 nm resolution, Sci. Rep. 1 (175) (2011) http://dx.doi.org/10.1038/srep00175.
[7] F.K. Chun, C.C. Shu, Dynamic control of the interference pattern of surface plasmon polaritons and its application to particle manipulation, Opt. Express 26 (15) (2018) 19123–19136, http://dx.doi.org/10.1364/OE.26.019123.
[8] K.A. Willets, R.P. Van Duyne, Localized surface plasmon resonance spectroscopy and sensing, Annu. Rev. Phys. Chem. 58 (2007) 267–297, http://dx.doi.org/10.1146/annurev.physchem.58.032806.104607.
[9] J. Homola, S.S. Yee, G. Gauglitz, Surface plasmon resonance sensors:review, Sensors Actuators B 54 (3) (1999) 15, http://dx.doi.org/10.1016/S0925-4005(98)00321-9.
[10] H. Wei, S. Zhang, X. Tian, H. Xu, Highly tunable propagating surface plasmons on supported silver nanowires, Proc. Natl. Acad. Sci. 110 (12) (2013) 4494–4499, http://dx.doi.org/10.1073/pnas.1217931110.
[11] J. Takahara, S. Yamagishi, H. Taki, A. Morimoto, T. Kobayashi, Guiding of a one-dimensional optical beam with nanometer diameter, Opt. Lett. 22 (1997) 475–477, http://dx.doi.org/10.1364/OL.22.000475.
[12] J. Burke, G. Stegeman, T. Tamir, Surface-polaritonlike waves guided by thin, lossy metal films, Opt. Lett. 87 (1983) 383–385, http://dx.doi.org/10.1364/OL.8.000383.
[13] J. Chen, C. Wang, G. Lu, W. Li, J. Xiao, Q. Gong, Highly efficient nanofocusing based on a t-shape micro-slit surrounded with multi-slits, Opt. Express 20 (17734) (2012) http://dx.doi.org/10.1364/OE.20.017734.
[14] W. Chen, D.C. Abeysinghe, R.L. Nelson, Q. Zhan, Plasmonic lens made of multiple concentric metallic rings under radially polarized illumination, Nano Lett. 9 (4320) (2009) http://dx.doi.org/10.1021/nl903145p.
[15] J.M. Yi, A. Cuche, E. Devaux, C. Genet, T.W. Ebbesen, Beaming visible light with a plasmonic aperture antenna, ACS Photonics 1 (365) (2014) http://dx.doi.org/10.1021/ph400146n.
[16] R. Peng, X. Li, Z. Zhao, C. Wang, M. Hong, X. Luo, Super-resolution long-depth focusing by radially polarized light irradiation through plasmonic lens in optical meso-field, Plasmonics 9 (2014) 55, http://dx.doi.org/10.1007/s11468-013-9597-8.
[17] C. Genet, T.W. Ebbesen, Light in tiny holes, Nature 445 (39) (2007) http://dx.doi.org/10.1038/nature05350.
[18] I.P. Radko, S.I. Bozhevolnyi, G. Brucoli, L. Martín-Moreno, F.J. García-Vidal, A. Boltasseva, Efficient unidirectional ridge excitation of surface plasmons, Opt. Express 17 (9) (2009) 7228, http://dx.doi.org/10.1364/OE.17.007228.
[19] S.B. Raghunathan, C.H. Gan, T.V. Dijk, B.E. Kim, H.F. Schouten, W. Ubachs, P. Lalanne, T.D. Visser, Plasmon switching: observation of dynamic surface plasmon steering by selective mode excitation in a sub-wavelength slit, Opt. Express 20 (14) (2012) 15326–15335, http://dx.doi.org/10.1364/OE.20.015326.
[20] F. Lu, F. Xiao, K. Li, A.S. Xu, Ultra-broadband wide-angle unidirectional plasmonic coupler based on joint effects of plasmonic critical angles and subwavelength metallic gratings, Opt. Lett. 39 (11) (2014) 3254–3257, http://dx.doi.org/10.1364/OL.39.003254.
[21] X.W. Li, Q.F. Tan, B.F. Bai, G.F. Jin, Experimental demonstration of tunable directional excitation of surface plasmon polaritons with a subwavelength metallic double slit, Appl. Phys. Lett. 98 (25) (2011) 824, http://dx.doi.org/10.1063/1.3602322.
[22] C.F. Kuo, S.C. Chu, Launching of surface plasmon polaritons with tunable directions and intensity ratios by phase control of dual fundamental Gaussian beams, Opt. Express 25 (9) (2017) 10456, http://dx.doi.org/10.1364/OE.25.010456.
[23] X. Huang, M.L. Brongersma, Compact aperiodic metallic groove arrays for unidirectional launching of surface plasmons, Nano Lett. 13 (11) (2013) 5420, http://dx.doi.org/10.1021/nl402982u.
[24] M. Janipour, F.H. Kashani, Directional radiation of surface plasmon polaritons at visible wavelengths through a nanohole dimer optical antenna milled in a gold film, J. Opt. Soc. Korea 18 (6) (2014) 799–808, http://dx.doi.org/10.3807/JOSK.2014.18.6.799.
[25] W. Yao, S. Liu, H. Liao, Z. Li, C. Sun, J. Chen, Q. Gong, Efficient directional excitation of surface plasmons by a single-element nanoantenna, Nano Lett. 15 (5) (2015) 3115, http://dx.doi.org/10.1021/acs.nanolett.5b00181.

[26] X. Zhang, Z. Li, J. Chen, Q. Gong, A dichroic surface-plasmon-polariton splitter based on an asymmetric T-shape nanoslit, Opt. Express 21 (12) (2013) 14548–14554, http://dx.doi.org/10.1364/OE.21.014548.

[27] S. Palomba, Y. Liu, Y. Park, T. Zentgraf, X. Yin, X. Zhang, Compact magnetic antennas for directional excitation of surface plasmons, Nano Lett. 12 (9) (2012) 4853, http://dx.doi.org/10.1021/nl302339z.

[28] R. Dom, S. Quabis, G. Leuchs, Sharper focus for a radially polarized light beam, Phys. Rev. Lett. 91 (23) (2003) 233901, http://dx.doi.org/10.1103/PhysRevLett.91.233901.

[29] K.J. Moh, X.C. Yuan, J. Bu, S.W. Zhu, B.Z. Gao, Surface plasmon resonance imaging of cell substrate contacts with radially polarized beams, Opt. Express 16 (20734) (2008) 20734–20741, http://dx.doi.org/10.1364/OE.16.020734.

[30] G. Terakado, H. Kano, K. Watanabe, Localized surface plasmon microscope with an illumination system employing a radially polarized zeroth-order bessel beam, Opt. Lett. 34 (8) (2009) 1180–1182, http://dx.doi.org/10.1364/OL.34.001180.

[31] Z.S. Man, L.P. Du, C.J. Min, Y.Q. Zhang, C.L. Zhang, S.W. Zhu, H.P. Urbach, X.C. Yuan, Dynamic plasmonic beam shaping by vector beams with arbitrary locally linear polarization states, Appl. Phys. Lett. 105 (011110) (2014) 2091, http://dx.doi.org/10.1063/1.4887824.

[32] J.J. Stmnes, Waves in Focal Regions, Adam Hilger, Bristol, UK, 1986.

[33] X.L. Wang, B.W. Zhu, Y.X. Dong, S. Wang, Z.Q. Zhu, F. Bo, X.P. Li, Generation of equilateral-polygon-like flat-top focus by tightly focusing radially polarized beams superposed with off-axis vortex arrays, Opt. Express 25 (22) (2017) 26844–26852, http://dx.doi.org/10.1364/OE.25.026844.